16th World Conference on Earthquake, 16WCEE 2017
Santiago Chile, January 9th to 13th 2017
Paper N° 2513
Registration Code: S-418974651

PERFORMANCE EVALUATION OF SUPERELASTIC VISCOUS DAMPERS CONSIDERING TEMPERATURE EFFECTS

B. Silwal[(1)], O.E. Ozbulut[(2)], R.J. Michael[(3)]

[(1)] PhD Student, Department of Civil and Environmental Engineering, University of Virginia, Charlottesville, Virginia, USA, E-mail: b@virginia.edu

[(2)] Assistant Professor, Department of Civil and Environmental Engineering, University of Virginia, Charlottesville, Virginia, USA, E-mail: ozbulut@virginia.edu

[(3)] Assistant Professor, Department of Mechanical Engineering, Gannon University, Erie, Pennsylvania, USA

Abstract

This paper investigates the seismic performance of a hybrid damper, named as superelastic viscous damper (SVD), considering environmental temperature changes. The SVD relies on shape memory alloy (SMA) elements for re-centering capability and employs a viscoelastic (VE) damper to augment its energy dissipation capacity. The VE damper consists of two layers of a high damped (HD) blended butyl elastomer compound, sandwiched between and bonded to three identical steel plates. Experimental tests at different temperatures are conducted on SMA elements and HD butyl elastomer to characterize their temperature dependent behavior. A nine-story steel frame building is designed and modeled with SVDs in OpenSees. Nonlinear time history analyses of the steel frame building with installed SVDs are conducted for outside temperatures of 0°C, 23°C and 40°C. A total of 10 far-field ground motion records are employed in the simulations. The variation of peak interstory drift ratio, which is correlated with damage in structural elements, and peak absolute floor acceleration, which is correlated with damage in non-structural components, with temperature are studied. The results show that for the structures designed with SVDs a decrease in temperature below room temperature will produce smaller peak story drift and floor accelerations, while an increase in temperature above room temperature will cause an increase in the peak response quantities of the structure. However, it is shown that this increase is not significant and limited to about 10%.

Keywords: shape memory alloys; viscoelastic damper; seismic; passive control; temperature effects

1. Introduction

Shape memory alloys (SMAs) have received considerable attention for civil engineering applications since early 2000. When an SMA is deformed up to certain strain level (about 6-8%), it can recover large deformations upon unloading. This recovery is due to the solid-to-solid phase transformations and is called as superelasticity. Although the material returns to its original shape when the load is removed, the loading trajectory and unloading trajectory does not coincide, leading to a hysteretic behavior.

Due to their excellent self-centering behavior as well as energy dissipation capability resulting from hysteretic behavior, a number of researchers have investigated the use of SMAs for mitigating response of structures subjected to earthquakes [1]. Various implementation techniques and strategies have been proposed for the use of SMAs in seismic applications [2-5]. One such a technique is the installation of SMA-based passive control devices into structures. The main goal in development of SMA-based control devices is to achieve flag-shaped hysteretic systems that can provide stable energy dissipation and satisfactory re-centering response within a design deformation. Since the equivalent viscous damping provide by SMAs is limited to 3-5% at dynamic loading rates [6], researchers have investigated the development of hybrid devices that employ SMAs for mainly re-centering purposes and an energy dissipative device for improving damping capacity [7-12].

Superelastic viscous damper (SVD), proposed by Silwal et al. [13], is a hybrid passive control device that strategically combines a viscoelastic device and shape memory alloys in parallel. The device consists of two high damped butyl elastomer compounds, sandwiched between and bonded to three identical steel plates and

installed SMA elements as shown in Fig. 1. SMA elements are wrapped around the outer two plates, forming a continuous loop. Along the top and bottom of the device, the SMA elements are threaded through guides, which ensure that the SMAs remain parallel to the direction of shear deformation in the elastomer layers. Whether the device itself moves left or right, the configuration ensures that the SMA elements will remain under tension. The viscoelastic component of the SVD compromises high damped butyl rubber, which is an elastomer specifically compounded to produce maximum damping at minimum stiffness. The effectiveness of SVDs in mitigating seismic response of steel moment resisting frames was shown in a previous study [13]. However, since the mechanical behavior of SMAs and butyl rubber is highly dependent on temperature, it is important to study the effect of temperature on the performance of SVDs.

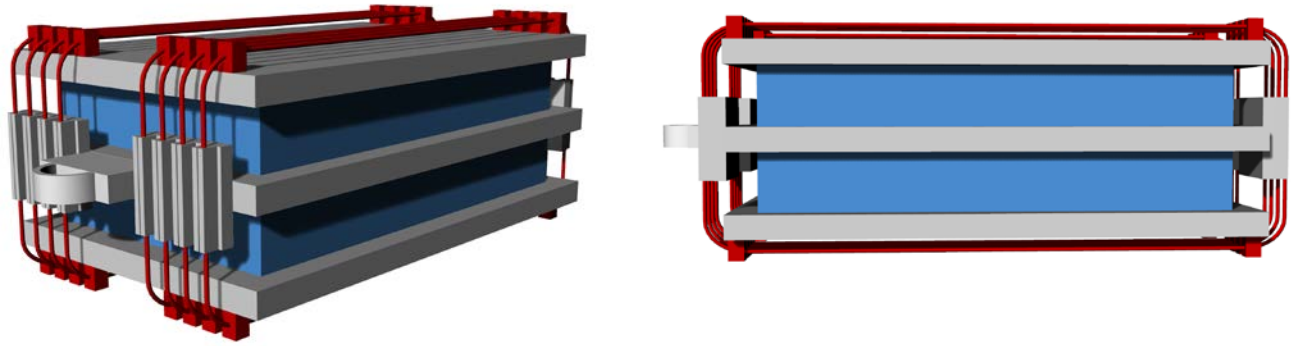

Fig. 1 – Superelastic viscous damper

This paper explores seismic performance of SVDs considering environmental temperature changes. First, the influence of temperature on hysteretic response of butyl rubber and SMAs are discussed through experimental test results. Then, a nine-story steel moment-resisting frame building is designed with SVDs. Numerical models of the building and SVDs are developed in a finite element program. Nonlinear response time history analyses are conducted at three different temperatures under 10 ground motion records. Results are analyzed in terms of peak story drift and peak absolute acceleration.

2. Temperature Effects on Butyl Rubber

Butyl rubber is a synthetic rubber produced by polymerization of about 98% isobutylene with about 2% of isoprene. Butyl rubber is also known as polyisobutylene or PIB. It has excellent impermeability, inherently high damping and its long polymer chains give it excellent flex properties. The first major application of butyl was tire inner tubes because of its excellent impermeability to air. Butyl is also used extensively in vibration isolators due to its high damping [14-15]. Other favorable properties include a low glass transition temperature, low modulus, low compression set and excellent resistance to aging and to weathering from atmospheric exposure.

The HD butyl compounds developed and used in this study are highly loaded which means that the % rubber hydrocarbon (rhc) is lower than traditional industrial butyls. Since there is less elastomer in it, the damping tends to go up because carbon black and oil, the typical materials used to lower the rhc, generally have higher damping than the rubber alone. In addition, these compounds utilize a grade of carbon black that builds hardness slowly so in order to get an equivalent hardness to the industrial butyl, for instance, more carbon black is needed which tends to drive up the damping. Also these compounds use a higher viscosity plasticizer which tends to drive up damping even more.

Perhaps the biggest difference between the HD butyl and industrial butyl is in the curative package. The HD butyl formula has a much stronger vulcanization package, which results in a much higher crosslink density and therefore, a somewhat stiffer elastic matrix. But the energy dissipating mechanisms of the black and the oil remain constant and may also increase with the more complex cure state, so the ratio of elastic to damping mechanisms shifts towards the damping, and loss factor jumps as a result.

In order to assess the effect of temperature on the behavior of HD butyl rubber, static and dynamic shear tests were conducted. The HD butyl was 50 durometer Shore A. All tests were performed according to ASTM D5992. The specimen geometry was a double shear with two identical rubber elements symmetrically disposed on opposite sides of a central rigid member. This specimen geometry was specified in ASTM D5992 and carefully designed to yield a length/wall thickness ratio of 8 (=1.6"/.2") to achieve a state of pure shear. All testing is performed on an MTS 810 servo-hydraulic test system. An environmental chamber was used to create desired test temperatures.

The tests were conducted at 100% shear strain at 1 Hz loading frequency. This strain level was selected to yield useful information about temperature impact as higher strain levels tend to be dominated by nonlinear effects. The tests were performed at 0ºC, 23ºC and 40ºC. Fig. 2 shows the hysteresis loops at various temperatures for the HD butyl rubber. In addition, to enable the evaluation of the test results in a quantitative way, the equivalent stiffness and loss factor were calculated. They are defined as:

$$K_s = \frac{F_{max} - F_{min}}{d_{max} - d_{min}} \tag{1}$$

$$\eta = \frac{1}{2\pi}\frac{E_D}{E_S} \tag{2}$$

where E_D is the energy dissipated per cycle (hysteresis area), E_S is the maximum strain energy for the same cycle calculated as the energy absorbed in a linear system that has the same maximum displacement and force, F_{max} and F_{min} are the maximum and minimum forces attained for the maximum and minimum cyclic displacements d_{max} and d_{min}. Fig. 3 illustrates the variation of equivalent stiffness and loss factor with temperature. The results reveal that both the equivalent stiffness and loss factor decreases with increasing temperature. The properties seem to be more temperature sensitive when the temperature decreases below room temperature compared to an increase in temperature above room temperature. In particular, the equivalent stiffness and loss factor vary +21% and +125%, respectively when the temperature changes from room temperature to 0ºC. On the other hand, the change in the equivalent stiffness and loss factor are only -13% and -23% when the temperature is increased from 23ºC to 40ºC.

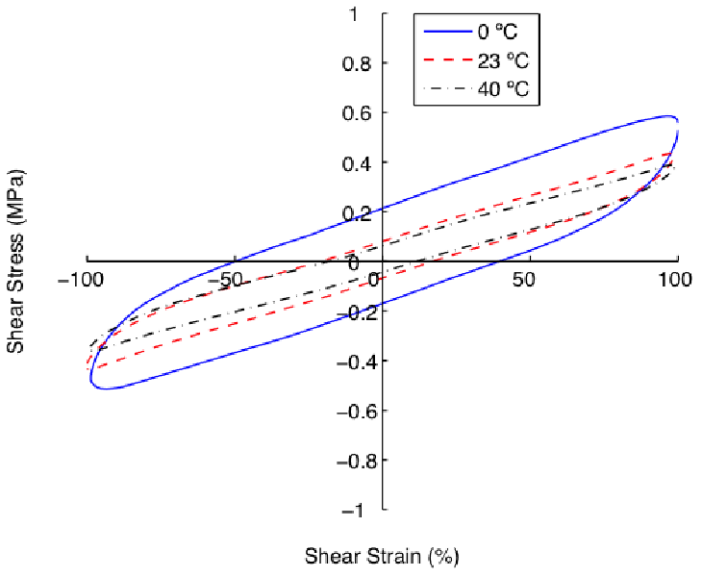

Fig. 2 – Shear stress – shear strain curves of HD butyl rubber at different temperatures

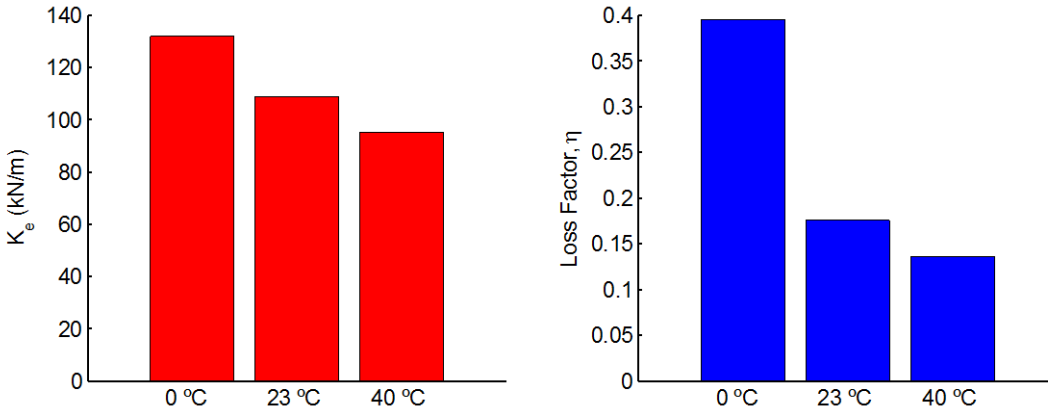

Fig. 3 – Variation of equivalent stiffness and loss factor for HD butyl with temperature

3. Temperature Effects on Shape Memory Alloys

In order to investigate the temperature dependence of superelastic behavior of NiTi SMAs, the experimental tests were conducted at different temperatures. The material used was NiTi wires with a diameter of 1.5 mm and obtained from SAES Smart Materials. The alloy chemical composition has 55.8% nickel by weight and the balance titanium. The austenite start and finish temperatures are specified by manufacturer as A_s = -10ºC and A_f = 5°C, respectively. An MTS servo-hydraulic load frame was used to conduct tests at various frequencies and temperatures. The sinusoidal tensile tests were performed under displacement control at 1 Hz at 0ºC, 23ºC and 40ºC. Fig. 4 shows strain-stress curves of NiTi wires at different temperatures. It can be seen that the hysteresis loops of SMA shifts upward with increasing temperature. Fig. 5 illustrates the variation of modulus of elasticity and loss factor with temperature. It can be seen that the modulus of elasticity decreases from 42.6 GPa at 23ºC to 27.6 GPa at 0ºC, recording a large decrease (-35%) in modulus of elasticity at low temperatures. However, the modulus varies only +10% when the temperature changes from 23ºC to 40ºC. On the other hand, the loss factor attains higher values at lower temperatures. As temperature increases from 0 ºC to 40 ºC, the loss factor reduces 38%. If the room temperature is considered as reference, the loss factor varies -24% at 0 ºC and +21% at 40 ºC.

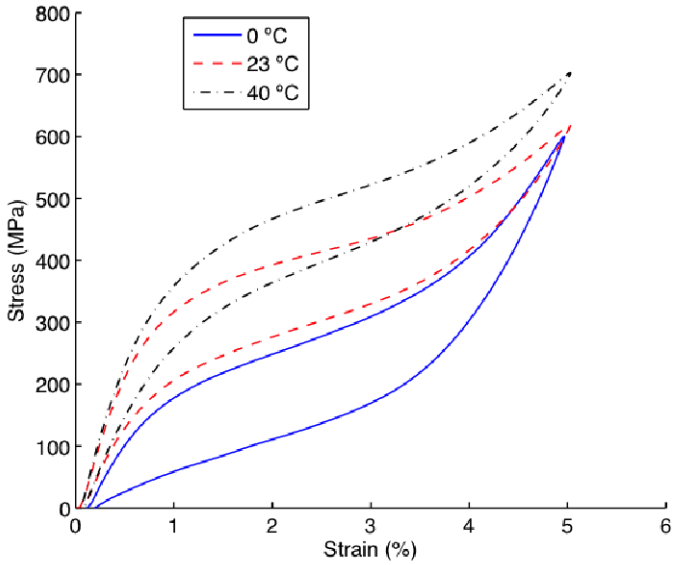

Fig. 4 – Stress – strain curves of SMAs at different temperatures

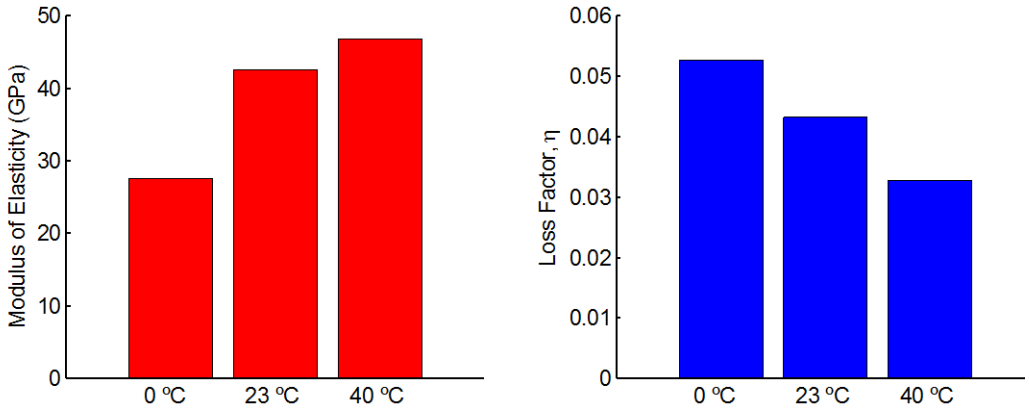

Fig. 5 – Variation of equivalent stiffness and loss factor for SMA with temperature

4. Building Description

A nine-story steel building is selected from the SAC steel project [16] for numerical analyses. The selected building includes a basement level in addition to the nine stories above the ground level and was originally designed as an office building located on a stiff-soil site (Site Class D) in Seattle, Washington. A floor plan and elevation of the nine-story building are shown in Fig. 6. The building has five bays at 9.15 m (30 feet) in each direction. The story height is 3.96 m (13 feet) at each floor except the first floor, which has a height of 5.49 m (18 feet) and the basement, which has a height of 3.65 m (12 feet). The lateral load resisting system in both directions consists of two special moment-resisting frames on the perimeter of the building. This study analyzes one of the moment frames in the E-W direction. The seismic masses are assigned as 1.01×10^6 kg for floor level 2, 9.89×10^5 kg for floor levels 3-9, and 1.07×10^6 kg for roof level. All the columns are assumed to be pinned at the base. The exterior columns at the ground level are also restrained laterally.

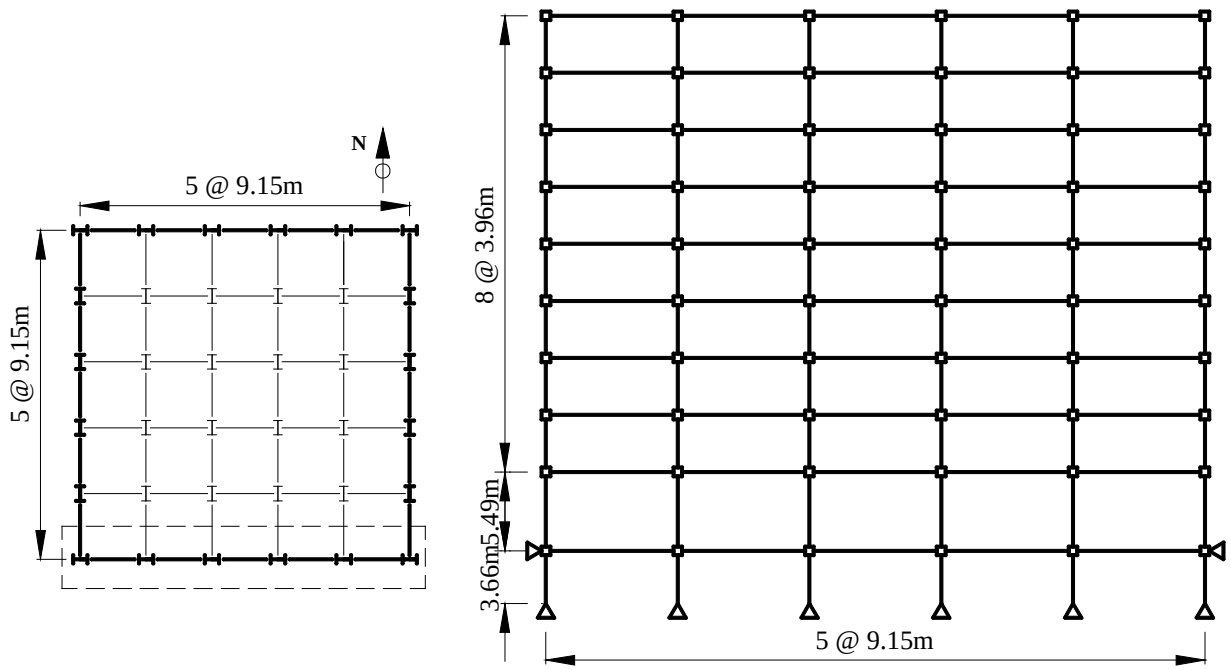

Fig. 6 – Plan and elevation of nine-story steel special moment resisting frame

The building is designed according to ASCE 7-10 [17] as a Risk Category II building by using nonlinear response history procedure. Based on the Seismic Design Category (SDC) D, the following design response spectral values are assigned to the site: S_{DS} = 0.912 g and S_{D1} = 0.530 g for the design basic earthquake (DBE), and S_{MS} = 1. 368 g and S_{M1} = 0.795 g for the maximum considered earthquake (MCE). Using the site's spectral acceleration values, the target spectra for the DBE and MCE levels are developed. A total of 7 ground motions is selected from PEER NGA database for the design and scaled according to ASCE 7-10. The steel members of the nine-story building are selected in accordance with the strength requirements of ANSI/AISC 360-10 [18] under the load combinations provided in ASCE 7-10. The building is also designed to comply with the drift requirements of ASCE 7-10. Since a nonlinear response history is adopted for the design, the allowable story drift is increased by 25% and determined from ASCE 7-10 for Risk Category II buildings as 2.5% under DBE level and as 3.75% under MCE level. The selected column and beam sections for the nine-story frame are shown in Table 1. The building satisfies the drift requirements under both DBE and MCE levels.

In order to design the nine-story frame with SVDs, a reduced strength version of the fully code compliant frame is developed first. In particular, the beam and column member sizes are reduced such that the steel frame satisfies the strength requirements of the design codes but does not meet the drift limits. In this more flexible frame, the added dampers will carry a larger portion of the seismic loads and will be mainly responsible to control the story drifts. Table 1 provides the selected member sizes for the reduced strength frame. The reduced strength steel frame is first upgraded with SVDs to comply with the story drift requirements of ASCE 7-10. For this study, the dimension of each elastomer compound of the SVD is selected to be 406×406×50 mm. The cross-sectional area and length of SMA elements for each SVD are selected to be 8 mm^2 and 1407 mm. With the selected parameters, the SVD has a design displacement of 100 mm and a maximum force capacity of 340 kN. The steel frame with SVDs is designed using the nonlinear response history procedure and following the seismic design requirements for structures with damping systems described in Chapter 18 of ASCE 7-10. The SVDs are installed at the second and fourth bay of each story level using a chevron brace configuration. From the nonlinear time history analyses, the number of dampers for each story is selected to be 8 to meet the drift requirements.

Table 1. Members of steel moment resisting frames

Story	SMRF with SVD		
	Exterior Columns	Interior Columns	Girders
1	W18x311	W18x311	W21x201
2	W18x311	W18x311	W21x201
3	W18x283	W18x283	W21x182
4	W18x283	W18x283	W21x182
5	W18x234	W18x234	W21x192
6	W18x234	W18x234	W21x192
7	W18x192	W18x192	W18x143
8	W18x192	W18x192	W18x143
9	W18x143	W18x143	W18x130
R	W18x143	W18x143	W18x130

5. Numerical Modeling

The numerical model of the nine-story steel frame building is developed in 2D using nonlinear seismic analysis program OpenSees. Based on the concentrated plasticity concept, the beam and column elements are modeled with elastic beam column elements connected by zero-length inelastic plastic hinges employing the

modified Ibarra-Krawinkler deterioration model [19]. The modified Ibarra-Krawinkler deterioration model considers bilinear hysteric response behavior. The cyclic deterioration model parameters of the zero-length rotational springs are assigned based on the model parameters developed by Lignos and Kwawinkler [20]. The deterioration characteristics of the rotational springs are indicated by yield strength, post-capping strength, unloading stiffness, and reloading stiffness. The moment-rotation curve is characterized by the elastic stiffness, plastic rotation, a post-capping plastic rotation capacity and the corresponding residual strength. The yield stress of structural steel is assumed to be equal to 375 MPa. To capture the important panel zone deformation modes, the panel zones are modeled considering the shear distortion in beam-column joints using Krawinkler model [21]. The Krawinkler model includes four rigid links and a rotational spring at the upper right corner to represent shear distortion in the panel zone. The nonlinear plastic hinges are created in beams at an offset from the interface of the panel zone and the beam element while the column plastic hinges are assigned at the face of the panel zone and the column element. To account for P-delta effects, a leaning column is linked to each model with elastic beam-column elements and connected to the model with an axially rigid truss element at each story level. The model assumes Rayleigh damping with a 2% damping ratio for the first and third modes.

The model of the superelastic viscous damper is developed in OpenSees by combining a finite length element with uniaxial self-centering material and elastic multilinear material property to represent the SMAs and a zero-length element with the Maxwell material property to model the elastomeric compound. The SMA behavior is accurately captured by a series combination of two uniaxial material models: SelfCentering material and ElasticMultiLinear material. The self-centering material exhibits flag-shaped hysteric response and captures the post-transformation hardening behavior with a post-hardening stiffness equals to the initial stiffness, whereas the elastic multilinear material accounts for the intial slackness in the SVD. Fig. 7 illustrates the parameters needed to define self-cenetering and Maxwell material properties. The experimental test results at different temperatures on SMAs and HD butyl compound are used to develop model parameters for the SMA and elastomeric compound. The selected parameters for each temperature are shown in Table 2.

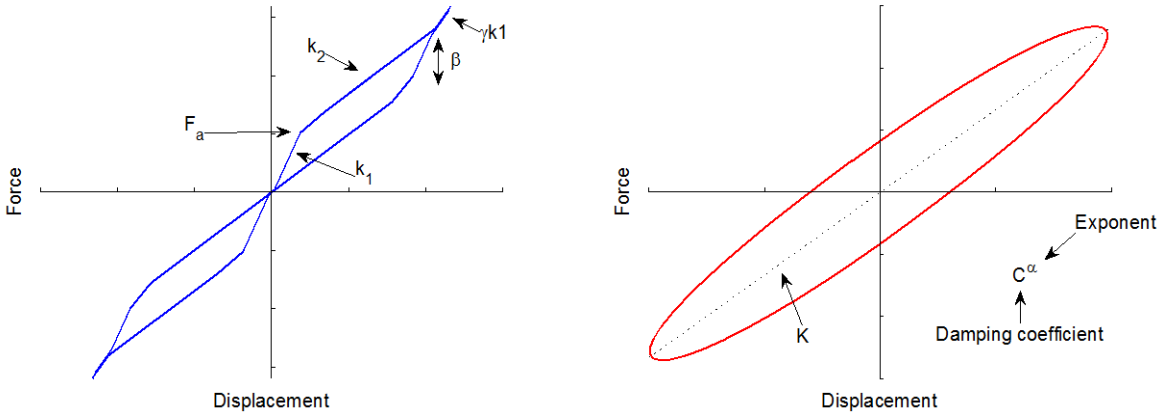

Fig. 7 – Parameters used to model SMA wires and butyl rubber in OpenSees

Table 2. Model parameters for butyl rubber and SMAs for different temperatures

Temperature	Butyl rubber			SMA				
	K (kN/mm)	C (kN-s/mm)	α	k_1 (kN/mm)	k_2 (kN/mm)	γ	F_a (kN)	β
0ºC	2.15	0.92	0.8	2.03	1.07	1.4	46.26	1
23ºC	1.43	1.00	0.8	3.12	0.969	1.2	71.17	0.5
40ºC	1.22	1.01	0.8	3.59	1.24	1.2	81.99	0.389

6. Nonlinear Response History Analysis

To evaluate effect of temperature on the performance of SVDs in mitigating the seismic response of steel frame structures, nonlinear response time history analyses are conducted for the steel frame with SVDs at different temperatures. The response of steel frame is evaluated under two different hazard levels: the design basis earthquake (DBE) seismic hazard level with a probability of exceedance of 10% in 50 years and the maximum considered earthquake (MCE) seismic hazard level with a probability of exceedance of 2% in 50 years. A total of 10 ground motion records that are also used in the FEMA P695 [22] methodology is employed for nonlinear time history analyses. Table 3 provides the characteristics of the selected ground motion records. The records are collectively scaled to selected hazard level, as defined in ASCE/SEI 7-05, such that the median spectral acceleration of the record set matches with those of the design spectra at the fundamental period of steel moment resisting frame.

Table 3. Ground motion records used in analyses

No.	Earthquake	Station Name	Component	Magnitude (M_w)	Distance (km)	Peak Ground Acceleration (g)	Peak Ground Velocity (cm/s)
1	Northridge (1994)	Beverly Hills-Mulhol	MUL009	6.7	13.3	0.42	59
2	Northridge (1994)	Beverly Hills-Mulhol	MUL279	6.7	13.3	0.52	63
3	Northridge (1994)	Canyon Country-WLC	LOS000	6.7	26.5	0.41	43
4	Northridge (1994)	Canyon Country-WLC	LOS270	6.7	26.5	0.48	45
5	Duzce, Turkey (1999)	Bolu	BOL000	7.1	41.3	0.73	56
6	Duzce, Turkey (1999)	Bolu	BOL090	7.1	41.3	0.82	62
7	Hector Mine (1999)	Hector	HEC000	7.1	26.5	0.26	29
8	Hector Mine (1999)	Hector	HEC090	7.1	26.5	0.34	42
9	Imperial Valley (1979)	Delta	H-DLT262	6.5	33.7	0.24	26
10	Imperial Valley (1979)	Delta	H-DLT352	6.5	33.7	0.35	33

Structural responses of the uncontrolled building and the building with installed hybrid dampers are computed under each ground motion record at two seismic hazard levels. The distribution of the peak interstory drift and peak floor acceleration over the height of the building are computed for the steel frame with installed SVDs at different temperatures. Median response of ten records for each temperature at the DBE level and MCE level is provided in Figs. 8 and 9, respectively. It can be seen that the SVD system has the lowest interstory drift and acceleration response values at both the DBE and MCE levels when the temperature is 0ºC. This can be attributed to the fact that the damping ratio for both butyl rubber and SMAs increases with a decrease in temperature. Also, the stiffness of the SMAs considerably decreases at 0ºC, which reduces overall stiffness of the SVDS device at lower temperatures and lead to a reduction in acceleration response. Since the energy dissipation capacity of both butyl rubber and SMAs is lower at 40ºC compared to 23ºC, the peak story drifts has

the largest values at 40ºC for the frame with SVDs. Due to the increase in SMA forces at 40ºC, the peak acceleration response is slightly higher at 40ºC compared to that at 23ºC. When the temperature drops from 23ºC to 0ºC, the median story drift at each floor changes between +1% and -18%, and the median floor accelerations experience a decrease between a minimum of 0.4% and a maximum of 19% under DBE and MCE level ground motions. On the other hand, when the temperature increases from 23ºC to 40ºC, the median story drift at each floor increases between 0.1% and 7%, and the median floor accelerations experience a varies between +2% and +11% under DBE and MCE level ground motions.

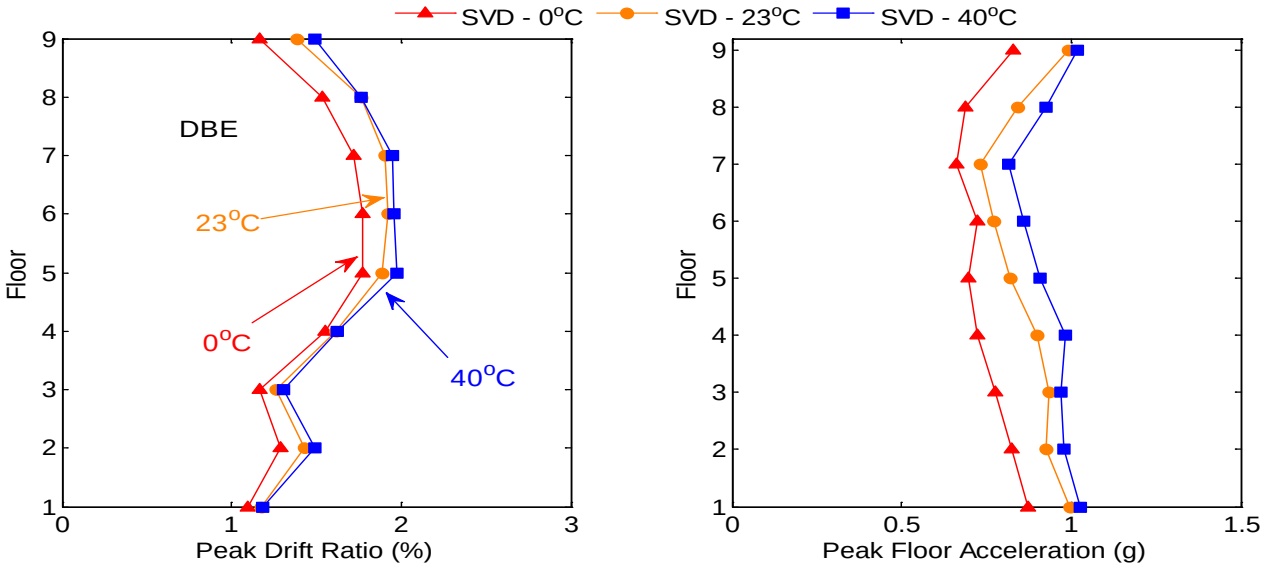

Fig. 8 – Envelopes for median of peak response quantities for SVD systems at different temperatures at DBE level hazard

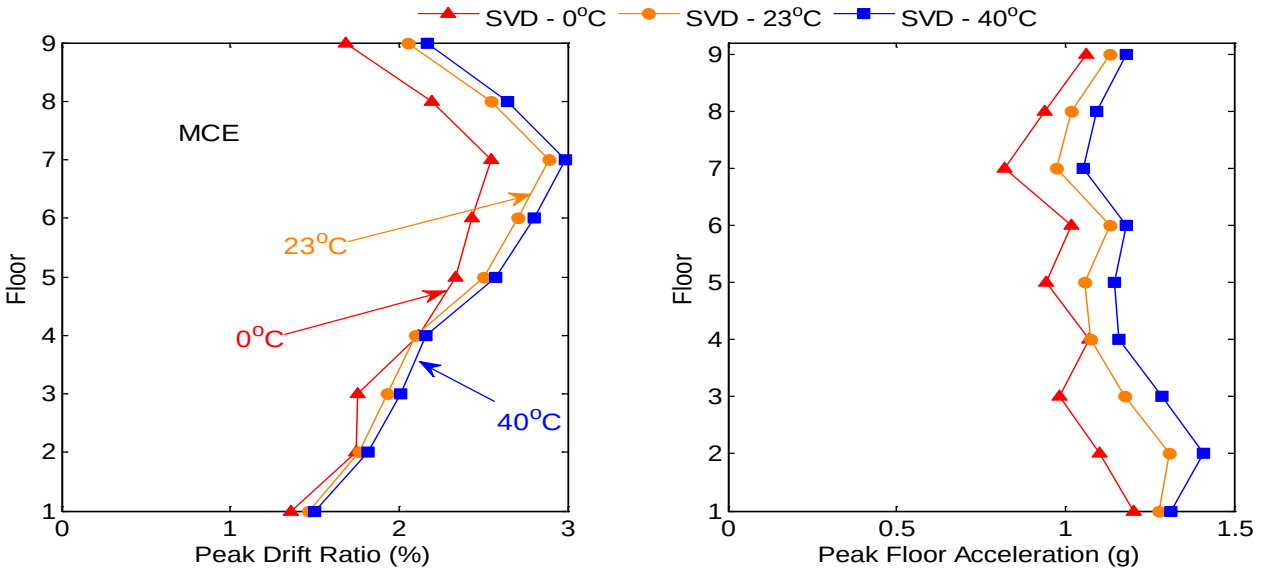

Fig. 9 – Envelopes for median of peak response quantities for SVD systems at different temperatures at MCE level hazard

In order to further evaluate the findings discussed above, Fig. 10 illustrates the force-displacement curves of all SVDs installed to the 6th floor at different temperatures. A larger hysteresis loop, which indicates more energy dissipation, is observed at 0ºC. Due to higher damping at 0ºC, peak story drifts attained their minimal values at that temperature. In addition, it can be seen that higher forces with larger stiffness are developed at 40ºC, which caused higher acceleration responses at high temperature.

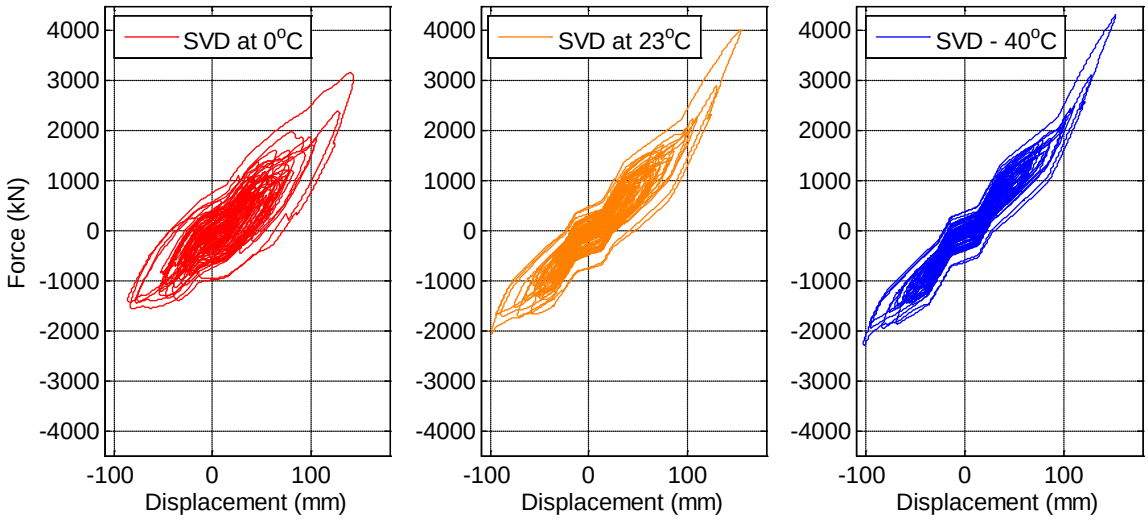

Fig. 10 – Force-displacement curves of SVDs at different temperatures under Imperial Valley earthquake

7. Conclusions

In this study, seismic performance of a nine-story steel moment resisting frame equipped with an SMA-based hybrid control device, named as superelastic viscous damper, is investigated under different temperatures. First, the effects of temperature on butyl rubber and SMAs are characterized through experimental testing. Then, a nine story steel moment resisting frame is designed with SVDs. Numerical models of both nine-story building and SVD device are generated in a finite element program. The parameters of SVD model are adjusted for three temperatures: 0ºC, 23ºC and 40ºC. Peak response quantities of the building are determined through nonlinear response history analyses at each temperature. Results shows that both peak story drift and peak floor acceleration have their minimal values at 0ºC, while larger responses are observed at 40ºC. Nevertheless, it is shown that designing structures with SVDs considering the room temperature material properties of SVDs will underestimate both the peak drift and acceleration response at various temperatures only about 10%.

8. References

[1] Ozbulut OE, Hurlebaus S, DesRoches R (2011): Seismic response control using shape memory alloys: A Review. *Journal of Intelligent Material Systems and Structures*, **22**, 1531-1549.

[2] Dezfuli FH, Alam MS (2013): Shape memory alloy wire-based smart natural rubber bearing. *Smart Materials and Structures*, **22**(4), 045013.

[3] Saiidi MS, Wang H (2006): Exploratory study of seismic response of concrete columns with shape memory alloys reinforcement. *ACI Structural Journal*, **103**(3), p.436.

[4] Ozbulut OE, Hurlebaus S (2011): Energy-balance assessment of shape memory alloy-based seismic isolation devices. *Smart Structures and Systems*, **8**, 399-412.

[5] Andrawes B, DesRoches R (2007): Comparison between shape memory alloy seismic restrainers and other bridge retrofit devices. *Journal of Bridge Engineering*,12(6), 700-709.

[6] Ozbulut OE, Hurlebaus S (2010) : Neuro-fuzzy modeling of temperature- and strain-rate-dependent behavior of NiTi shape memory alloys for seismic applications. *Journal of Intelligent Material Systems and Structures*, **21**, 837-849.

[7] Shook DA, Roschke PN, Ozbulut OE (2008): Superelastic semi-active damping of a base-isolated structure. *Structural Control & Health Monitoring*, **15**, 746-768.

[8] Miller DJ, Fahnestock LA, Eatherton MR (2012): Development and experimental validation of a nickel–titanium shape memory alloy self-centering buckling-restrained brace. *Engineering Structures*, **40**, 288-298.

[9] Ozbulut OE, Hurlebaus S (2012): Application of an SMA-based hybrid control device to 20-story nonlinear benchmark building. *Earthquake Engineering & Structural Dynamics*, **41**, 1831-1843.

[10] Ozbulut OE, Hurlebaus S (2012): Re-centering variable friction device for seismic control of structures. *Structural Longevity*, **7**, 29-36.

[11] Zhang Y, Zhu S (2007): A shape memory alloy-based reusable hysteretic damper for seismic hazard mitigation. *Smart Materials and Structures*, **16**(5), 1603.

[12] Speicher M, Hodgson DE, DesRoches R, Leon RT (2009): Shape memory alloy tension/compression device for seismic retrofit of buildings. *Journal of materials engineering and performance*, **18**(5-6), 746-753.

[13] Silwal B, Michael RJ, Ozbulut OE (2015): A superelastic viscous damper for enhanced seismic performance of steel frame structures. *Engineering Structures*, **105**, 152-164.

[14] Michael RJ, Johnson DH, Pollino M, Redovan J, Moser E, MacDonald B (2012): Development of a seismic isolation system for commercial storage racks. *In: International Mechanical Engineering Conference and Exposition*, Houston, TX 2012.

[15] Sweeney SK, Michael RJ (2006): Collaborative product realization of an innovative structural damper and application. *In: Proc. ASME International Mechanical Engineering Congress, IMECE2006*-13421, 1-9, Chicago, IL, November 2006.

[16] FEMA (2000): State of the art report on systems performance of steel moment frames subject to earthquake ground shaking, *SAC Joint Venture*.

[17] ASCE(2010): Minimum Design Loads for Buildings and Other Structures. ASCE 7-10, *American Society of Civil Engineers*, Reston, Virginia.

[18] AISC Committee (2010): Specification for Structural Steel Buildings (ANSI/AISC 360-10 : *American Institute of Steel Construction*, Chicago-Illinois.

[19] Ibarra LF, Medina RA, Krawinkler H (2005): Hysteretic models that incorporate strength and stiffness deterioration. *International Journal of Earthquake Engineering Structural Dynamics*, **34**(12): 1489-1511.

[20] Lignos DG, Krawinkler H (2007): A Database in Support of Modeling of Component Deterioration for Collapse Prediction of Steel Frame Structures. *Proc. ASCE Structures Congress, Long Beach*, California, May 18-20; 2007.

[21] Gupta A, Krawinkler H (1999): Seismic Demands for Performance Evaluation of Steel Moment Resisting Frame Structures. *Technical Report 132, The John A. Blume Earthquake Engineering Research Center*, Department of Civil Engineering, Stanford University, Stanford, CA.

[22] FEMA (2009): Quantification of building seismic performance factors. Report No. P695, *Federal Emergency Management Agency*, Washington, D.C.